Published in final edited form as:
*Circ Res*. 2010 April 2; 106(6): 1092–1102. doi:10.1161/CIRCRESAHA.109.215723.

# Plasminogen activator inhibitor-1 regulates myoendothelial junction formation

**Katherine Heberlein**[1,2], **Adam C. Straub, PhD**[1], **Angela K. Best**[1], **Mark A. Greyson**[1], **Robin C. Looft-Wilson, PhD**[3], **Poonam R. Sharma, PhD**[1], **Akshaya Meher, PhD**[1], **Norbert Leitinger, PhD**[1,4], and **Brant E Isakson, PhD**[1,2,*]

[1]Robert M. Berne Cardiovascular Research Center, University of Virginia School of Medicine, P.O. Box 801394, Charlottesville, VA 22908

[2]Department of Molecular Physiology and Biological Physics, University of Virginia School of Medicine

[3]Department of Kinesiology, College of William and Mary

[4]Department of Pharmacology, University of Virginia School of Medicine

## Abstract

**Rationale—**Plasminogen activator inhibitor-1 (PAI-1) is a biomarker for several vascular disease states; however, its target of action within the vessel wall is undefined.

**Objective—**Determine the ability of PAI-1 to regulate myoendothelial junction (MEJ) formation.

**Methods and Results—**Myoendothelial junctions are found throughout the vasculature linking endothelial cells (EC) and vascular smooth muscle cells (VSMC). Using a vascular cell co-culture (VCCC) we isolated MEJ fractions and performed two-dimensional differential gel electrophoresis. Mass spectrometry identified PAI-1 as being enriched within MEJ fractions, which we confirmed in vivo. In the VCCC, recombinant PAI-1 (rPAI-1) added to the EC monolayer significantly increased MEJs. Conversely, addition of a PAI-1 monoclonal antibody to the EC monolayer reduced the number of MEJs. This was also observed in vivo where mice fed a high fat diet had increased PAI-1 and MEJs and the number of MEJs in coronary arterioles of PAI-$1^{-/-}$ mice was significantly reduced when compared to C57Bl/6 mice. The presence of MEJs in PAI-$1^{-/-}$ coronary arterioles was restored when their hearts were transplanted into and exposed to the circulation of C57Bl/6 mice. Application of biotin-conjugated PAI-1 to the EC monolayer in vitro confirmed the ability of luminal PAI-1 to translocate to the MEJ. Functionally, phenylephrine-induced heterocellular calcium communication in the VCCC was temporally enhanced when rPAI-1 was present, and prolonged when PAI-1 was absent.

**Conclusion—**Our data implicate circulating PAI-1 as a key regulator of MEJ formation and a potential target for pharmacological intervention in diseases with vascular abnormalities (e.g., diabetes mellitus).

### Keywords

myoendothelial junction; plasminogen activator inhibitor-1; endothelial cell; smooth muscle cell

*to whom correspondence should be addressed, P: 434-924-2093, F: 434-924-2828, bei6n@virginia.edu.

**Disclosures**

None of the authors have any conflicts to disclose.

## Introduction

In diseases that exhibit vascular abnormalities, increased circulating plasminogen activator inhibitor-1 (PAI-1) is considered a major biomarker; however its function in these diseases remains unclear[1–5]. In the vasculature, fibrinolysis and the plasminogen activator (PA) system are regulated by PAI-1 through inhibition of urokinase PA (uPA) and tissue PA (tPA) [6, 7], maintaining an important balance between matrix degradation and cellular adhesion. Inhibition of PAs disrupts the activation of plasminogen into plasmin, negatively regulating localized matrix degradation and maintaining a stable scaffold for cells to adhere to[2, 8–10]. Decreases in PAI-1 results in excessive proteolytic activity and increased matrix degradation, creating an unstable extra cellular matrix (ECM) scaffold which disrupts cellular attachment and thereby the invasion by endothelial cell (EC) extensions into the ECM. Conversely, large increases in PAI-1 can inhibit overall matrix degradation, preventing the growth of EC extensions into the ECM[11, 12]. Therefore, the enzymatic balance of proteolytic activity and its regulation by PAI-1 is important in the formation of EC cellular extensions[11, 13, 14].

In the resistance vasculature, EC extensions that penetrate the ECM-rich internal elastic lamina (IEL) form myoendothelial junctions (MEJs), which are locations within a vessel where ECs establish heterocellular contact or apposition with vascular smooth muscle cells (VSMC)[15–17]. The MEJ is unique to the resistance vasculature and hypothesized to be a highly organized cell-signaling microdomain that facilitates heterocellular communication between EC and VSMC (for review see[18]). Several additional studies correlate changes in MEJ regulation with multiple vascular pathologies such as diabetes mellitus, where changes in the vasoreactivity of diseased vessels are associated with potential changes in the number of MEJs[18–21]. Despite the suggested importance of MEJs in the maintenance of vasomotor tone, there are currently no documented mechanisms regarding the regulation of MEJ formation and their potential role in vascular pathologies.

To test the hypothesis that PAI-1 can regulate MEJ formation we isolated in vitro MEJs and determined the enriched expression of PAI-1 at the MEJ and confirmed its presence at the MEJ in vivo. Modulation of PAI-1 activity at the EC luminal surface was reflected by changes in both in vitro and in vivo MEJ formation, where increases in PAI-1 augmented the number of MEJs and decreased PAI-1 activity had the opposite effect. Heterocellular communication between the two cell types, presumably occurring at the MEJ was also affected in response to changes in PAI-1 activity. We therefore suggest that circulating PAI-1 regulates MEJ formation and can alter heterocellular signaling mediated through MEJs in the resistance vasculature.

## Methods

Expanded methods are found in Supplementary section.

### Mice

Wildtype mice, strain C57Bl/6 and PAI-$1^{-/-}$ mice, strain B6.129S2-*Serpine1*$^{tm1Mlg}$/*J*, were males 8–10 weeks of age and used according to the University of Virginia Animal Care and Use Committee guidelines. Mice used for high fat comparison were C57Bl/6 mice fed a caloric-rich diet (5.45 kcal/g, 0.2% cholesterol, 35.5% fat; Bio-Serv). .

### Vascular cell-co-culture

Vascular cell co-cultures were assembled as described[22]. Cells were derived from human umbilical vein (Cell Applications, Inc, San Diego) and grown in M199 (Gibco) supplemented with 10% FBS (Gibco), 1% glutamine (Gibco), 1% penicillin/streptomycin (Gibco), EC media also contained endothelial cell growth supplement (5ug/mL, BD Biosciences); Additional cell

lines were derived from human coronary artery (Lonza, Walkersville). Endothelial cells were grown in EBM-2 MV (Lonza) supplemented with Lonza bullet kits (Lonza), VSMC were grown in SmBM (Lonza) supplemented with Lonza bullet kits (Lonza). Seeding densities of $7.5\times10^4$ VSMC and $3.6\times10^5$ EC were used.

Recombinant PAI-1 (rPAI-1; 0.1 μg/mL; Technoclone) and PAI-1 mAb (10 μg/mL; Technoclone) were added every 24 hours to ECs 48 hours before isolation. Biotin-conjugated rPAI-1 (Cell Sciences) was added to ECs 30 minutes before isolation.

### Isolation of MEJ fractions

Following 6 days in culture, VSMC monolayers were scraped into lysis buffer and repeated for EC monolayers. The MEJ fractions were collected by removing the denuded Transwell membranes into lysis buffer, and vortexing. All fractions were sonicated and spun at 2500 rpm for 5 minutes and the supernatant collected. All steps were performed at 4°C.

### Immunoblots

Protein fractions were run on 10% SDS-PAGE Gels, transferred to nitrocellulose and imaged on a Li-Cor Odyssey Imager[23].

### Antibodies and Protein

Secondary antibodies: phalloidin conjugated to Alexa 488 or Alexa 594, donkey anti-rabbit or donkey anti-mouse Alexa 488 or Alexa 594, all from Invitrogen. Goat anti-rabbit or anti-mouse IRDye 680 or 800CW was used for immunoblots (Li-cor Biosciences). Primary antibodies: SMα-actin (monoclonal, Sigma); VE-cadherin, uPA and tPA (all polyclonal, Santa Cruz Biotechnologies), GAPDH (monoclonal, Zymed), PAI-1 polyclonal (Abcam), PAI-1 monoclonal (immunoblot analysis, BD Biosciences), Cx37 and Cx40 (polyclonal, ADI), Cx43 (polyclonal, Sigma) Cx45 (polyclonal, kind gift of Steinberg, Washington University24), Anti-rabbit 10 nm gold beads were from Jackson Labs.

### 2D-DIGE Analysis

Individual protein fractions were labeled with Cy2, Cy3 or Cy5 and run per manufacturer specifications (Amersham BioSciences). IPG strips were transferred into gradient SDS-Gel (9–12% SDS). Image scans were made using Typhoon TRIO (Amersham BioSciences), analyzed by Image QuantTL software (GE-Healthcare). The ratio change of protein differential expression was obtained by in-gel DeCyder software analysis.

### Mass Spectrometry

Proteins of interest were digested in-gel and MALDI-TOF MS and TOF/TOF tandem MS/MS were performed. Peptide mass and associated fragmentation spectra were searched in the National Center for Biotechnology Information non-redundant (NCBInr) database. Candidates with protein score confidence interval percent (C.I.%) or Ion C.I.% greater than 95 were considered significant.

### Immunostaining

Immunohistochemistry on the VCCC was performed as described[22],

### Quantification of MEJs using the VCCC

The number of F-actin filled pores per micrometer was quantified using Metamorph (Universal Imaging Corps, version 7.5.6.0). Phalloidin staining visualized F-actin within pores of the Transwell.

### Immunolabeling on TEM Sections

Visualization of proteins by TEM was performed as described[25]. Quantification of electron-dense gold-beads was performed by immunolabeling for PAI-1 with minimum 5 TEM images per coronary arteriole, 10 μm apart. The areas of each component (EC, MEJ and VSMC) were quantified using Metamorph software calibrated to measuring area ($\mu m^2$). The EC and VSMC monolayers were traced from apical to basal lateral membrane. For MEJs, cellular extensions penetrating the IEL were defined by a line across the basal lateral membrane from which the MEJ originated, dissecting the junction from the monolayer, tracing the extension through the IEL to the base of the adjacent basal lateral membrane. The area inside these lines defined the area of the MEJ. The number of gold beads in each area (EC, MEJ or VSMC) was counted. Measurements represent the average number of beads per micron squared ± SE.

### Quantification of PAI-1 on actin bridges in vivo

Quantification of PAI-1 on actin bridges formed between EC and VSMC in vivo was performed as previously described[25].

### Ultrastructure Electron Microscopy

Coronary arterioles were fixed in 4% paraformaldehyde and 2% gluteraldahyde at 4°C and ultrastructural TEM images were obtained as described[3]. We quantified the total number of MEJs within a vessel using a minimum of 5 TEM images per coronary arteriole. To quantify the radial length of a vessel, a single line was traced along the EC basal lateral membrane with this distance measured using calibrated Metamorph software. Cellular extensions that penetrated the traced EC basal lateral membrane, IEL and came within <250 nm of membranous contact between EC and VSMC was counted as one MEJ. Numbers represent the average number of MEJs per 10 μm radial length ± SE. A minimum radial diameter of 150 mm per mouse and 10 μm between each TEM section were used.

### Heart Transplants

Heart transplants were performed as described[26], (see Supplementary Fig I). Five days post-surgery, donor hearts were harvested for TEM.

### Recombinant PAI-1 Tail Vein Injections

Fifty microliters (μL) of rPAI-1 (1000 ng/μg) or saline was injected into PAI-$1^{-/-}$ mice via lateral tail vein every 12 hours for five days. Tissue was harvested for TEM.

### Calcium Imaging

Fura-2 AM was loaded onto EC and VSMC monolayers as described for Fluo-4 AM[27], (see Supplementary Fig II). The VSMC were stimulated with 10 μmoles/L phenylephrine (PE) and EC intracellular calcium concentrations $[Ca^{2+}]_i$ were recorded as described[27].

### Statistics

Significance for all experiments was at $P<0.05$ and determined by one-way ANOVA (Bonferroni post hoc test); error bars are ±SE using Origin Pro 6.0 software.

## Results

### Isolation and characterization of myoendothelial junction proteins

For initial experiments demonstrating isolation of EC, VSMC and MEJ protein fractions we used phalloidin to mark cellular components of the VCCC. In Figure 1A, D, an intact VCCC with cell monolayers and actin extensions within the pores of the Transwell (e.g., in vitro

MEJs22) is clearly observed. The formation of junctions is also confirmed by expression of vascular specific connexins in isolated VSMC, EC and MEJ fractions (as previously described, eg.22, Supplementary Fig III). After the EC and VSMC monolayers were removed by scraping, the actin extensions within the Transwell pores remained (Fig 1B, E). When the scraped membranes were vortexed with lysis buffer, in vitro MEJs were no longer visible via phalloidin staining (Fig 1C, F). The three fractions were analyzed via silver stain (Fig 1G) and GelCode Blue (Fig 1H), demonstrating an abundance of proteins in each fraction. Immunoblots demonstrated labeling of MEJ and EC fractions for VE-Cadherin (Fig 1I) and SMα-actin labeling of VSMC and MEJ fractions (Fig 1J), with equivalent loading for all three fractions (Fig 1K). These data demonstrate our ability to isolate in vitro MEJs from the VCCC.

Simultaneous comparison of isolated in vitro VSMC, EC and MEJ fractions was performed using 2D-DIGE proteomic analysis. Representative images compare EC and VSMC fractions (Fig 2A, top), MEJ and VSMC fractions (Fig 2A, middle) and MEJ and EC fractions (Fig 2A, bottom) from the same gel. Gel images for each fraction were obtained and overlaid, allowing direct quantitative comparison between each fraction of the same spot. Using Qualitative DeCyder analysis, all spots with increased protein expression in the MEJ fraction were identified. Of these, three spots (arrows 1–3) of similar molecular weight and pH had greater than 2.5 fold increase in protein expression in the MEJ fraction as compared to VSMC and EC fractions (Fig 2A). Using DeCyder software, spots 1–3 are represented quantitatively as protein expression peaks, where each spot is identified by a magenta tracer (Fig 2B). Mass spectrometry identified each of these spots as PAI-1, with minimal 99.9% confidence in protein identification (Fig 2C). It is likely, although not confirmed that each spot represents a separate glycosylation isoform of PAI-1. Results were confirmed using coronary artery EC, VSMC and MEJ fractions (Supplementary Fig IV)

## PAI-1 at the MEJ

To verify expression of PAI-1 at the MEJ in vitro, we immunoblotted isolated VSMC, EC and MEJ fractions and showed enrichment of PAI-1 in MEJ fractions (Fig 3A). Using confocal microscopy to image transverse sections of the VCCC, we also confirmed the expression of PAI-1 in the pores of the VCCC membrane, where PAI-1 colocalized with F-actin regardless of it's location in the Transwell pores (Fig 3B). Associated substrates for PAI-1, active and inactive uPA, but not tPA, were increased in MEJ fractions (Supplementary Fig V), supporting our identification of PAI-1 at the MEJ in vitro. Quantified immunohistochemistry of whole mount tissue preps from fixed C57Bl/6 and PAI-$1^{-/-}$ mesenteric, cremasteric and coronary microvascular beds labeled for PAI-1 confirm the presence of PAI-1 on actin bridges in vivo (Fig 3C). Quantified immunolabeling for PAI-1 on TEM sections of C57Bl/6 coronary arterioles showed expression of PAI-1 at the MEJ in vivo (Fig 3D, as well as mesenteric and cremasteric arterioles, Supplementary Fig VI).

The presence of PAI-1 is crucial for invasion of EC extensions into the ECM[13]. To determine if PAI-1 is similarly necessary for the formation of MEJs, we depleted PAI-1 activity in each monolayer using a PAI-1 specific mAb or increased PAI-1 activity using rPAI-1. Depletion of activity caused a significant reduction in MEJs, but only when applied to EC or EC/VSMC monolayers (Fig 4A, Supplementary Fig VII). Likewise, addition of rPAI-1 caused a significant increase in MEJs only in the EC and EC/VSMC treated monolayers (Fig 4B, Supplementary Fig VII). The identification of PAI-1 was corroborated in coronary artery cells with immunoblots for PAI-1 at the MEJ as well as changes in MEJ formation in response to changes in PAI-1 (Supplementary Fig VII).

To verify the ability of PAI-1 to regulate MEJ formation in vivo, we performed TEM ultrastructure analysis on coronary arterioles isolated from C57Bl/6 and PAI-$1^{-/-}$ mice. Vessels from C57Bl/6 mice had significantly more MEJs (Fig 5A,I) than those from PAI-$1^{-/-}$ mice

(Fig 5B,I). This was also demonstrated in mesenteric and cremasteric arterioles (Supplementary Fig VIII). Conversely, coronary arterioles isolated from C57Bl/6 mice fed a high fat diet had increased PAI-1 expression (Supplementary Fig IX) and significantly more MEJs (Fig 5C,I) as compared to C57Bl/6 mice fed a standard chow diet. To test whether circulating PAI-1 could enhance MEJ formation in vivo, we performed heterotypic heart transplants. Transplantation of a C57Bl/6 heart into a C57Bl/6 mouse (Fig 5D) or a PAI-$1^{-/-}$ heart into a PAI-$1^{-/-}$ mouse (Fig 5E) produced no change in MEJ formation (Fig 5A-B,I respectively). However, PAI-$1^{-/-}$ hearts transplanted into a C57Bl/6 mouse, increased MEJ formation similar to that seen in C57Bl/6 mice (Fig 5F,I). This data further suggests that circulating PAI-1 interacts with ECs to influence formation of MEJs. To verify that increases in MEJ formation were due to increases in PAI-1, we injected saline or rPAI-1 into PAI-$1^{-/-}$ mice via tail vein, to increase circulating PAI-1 (Supplementary Fig X). Saline injected PAI-$1^{-/-}$ mice showed no change in MEJ formation (Fig 5G) when compared to non-injected PAI-$1^{-/-}$ (Fig 5A,B,I). Increases in circulating PAI-1 (injected rPAI-1) produced similar increases in MEJ formation (Fig 5H) as compared to those seen following the heart transplants and C57Bl/6 mice (Fig 5A,E,I) suggesting changes in MEJ formation are likely due to PAI-1.

To determine if exposing the EC luminal surface to increased PAI-1 could result in relocation of PAI-1 to the MEJ, we applied biotin-conjugated rPAI-1 to the VSMC or EC monolayers of the VCCC thirty minutes prior to isolation. Following application of biotin-conjugated rPAI-1 to the VSMC the rPAI-1 could not be detected with streptavidin in the MEJ fractions, nor in the controls (Fig 6A–D). However, when applied to the EC monolayer, the biotin conjugated rPAI-1 was readily detected at the MEJ (Fig 6A,B E). The sum of the data suggests that increased PAI-1 results in the movement of PAI-1 from the lumen to the MEJ.

### Effects of PAI-1 on $Ca^{2+}$ signaling at the MEJ

To test the functional effect of changes in the number of MEJs as a result changes in PAI-1 activity in vitro, we measured heterocellular $Ca^{2+}$ communication from the VSMC to the EC by stimulating VSMC with PE (Fig 7A). Following stimulation of the VSMC with PE, there were no changes in the maximum EC $Ca^{2+}$ response regardless of EC treatment with rPAI-1 (+rPAI-1) or mAb to PAI-1(−PAI-1). The addition of gap junction blocker glycyrrhetinic acid (+GA) or inhibiting MEJ formation through collagen coating of the Transwell (Supplementary Fig XI) significantly decreased the EC $Ca^{2+}$ response (Fig 7B). However, the addition of rPAI-1 to the EC monolayer resulted in a more rapid increase in EC $Ca^{2+}$ as compared to EC monolayers with depleted PAI-1 (−PAI-1; Fig 7C, D). None of the conditions altered the expression of vascular connexins at the MEJ (Supplementary Fig XII). These data suggest that PAI-1 can enhance heterocellular communication, which is likely a result of increased MEJ formation.

## Discussion

In the present study we provide evidence for the biomarker PAI-1 in the regulation of MEJ formation and function. Plasminogen activator inhibitor-1 is the major regulator of the PA system. Components of the PA system, uPA and tPA activate plasminogen to plasmin, which degrades ECM. Specifically, inhibition of uPA by PAI-1 decreases matrix degradation, maintaining a localized area of structured matrix scaffold to facilitate cellular invasion of EC extensions into the ECM[11, 28, 29]. Because of its role in the formation of cellular extensions and regulation of matrix degradation, disruption of the balance between PA components, namely changes in PAI-1 activity, can result in decreased cellular invasion. In the resistance vasculature, cellular invasion by the EC or VSMC is required for functional MEJs to form. The disruption of MEJ function has been indirectly implicated in vascular diseases such as

diabetes mellitus[19–21]; however, no studies regarding regulation of MEJ formation have been reported.

To identify regulatory proteins enriched at the MEJ, we developed a method for isolating in vitro MEJ fractions using the VCCC as an in vitro model of the MEJ[22, 27, 30]. Isolation of specific EC, VSMC and MEJ protein fractions was confirmed using immunoblot analysis for cell-type specific markers, which not only demonstrated successful isolation of each monolayer, but isolation of the EC and VSMC components of the MEJ as well. This is the first time that MEJs have been directly isolated, either in vivo or in vitro and we believe this method will enhance the capacity to investigate the function of MEJs. Although a method to isolate protein from MEJs in vivo would be ideal, thus far any method to isolate and characterize MEJs outside of immunohistochemistry, usually using TEM (e.g.,16), has proven elusive.

Using simultaneous 2D-DIGE analysis, we identified three spots representing proteins with increased expression in the MEJ (in vitro) as compared to EC and VSMC and using mass spectrometry these spots were determined to be PAI-1. Expression of PAI-1 at the MEJ was confirmed both in vitro using confocal microscopy and in vivo using TEM. Because all three spots from the 2D-DIGE were found at the same molecular weight but demonstrated different isoelectric focusing, it is possible that each spot represents one of the glycosylated isoforms of PAI-1[31]. It has been suggested that the glycosylation state of PAI-1 may be useful in determining the protein's origin32 and further investigation regarding the glycosylated isoforms of PAI-1 could provide insight for the origin of PAI-1 expressed at the MEJ in vivo.

Due to PAI-1's ability to regulate matrix degradation and cellular adhesion to the ECM, it is considered an integral component of EC invasion into the ECM[11]. We therefore tested the hypothesis that MEJ formation mimics EC invasion of the ECM as regulated by PAI-1. Using the VCCC, increases in PAI-1 activity (by addition of rPAI-1) promoted an increase in the number of actin extensions (i.e., in vitro MEJs) that formed. Conversely depletion of endogenous PAI-1 activity (using a mAb specific for PAI-1) decreased the number of actin extensions, suggesting PAI-1 plays a critical role in the formation of MEJs. Correlating with these data, TEM analysis of isolated PAI-$1^{-/-}$ arterioles demonstrated significantly less MEJs as compared to C57Bl/6 mice. Ultrastructure analysis also revealed a thicker IEL in the knockout vessels as compared to wildtype. These data are in agreement with recent evidence that shows PAI-$1^{-/-}$ cells exhibit increased collagen production, which correlates with an increase in TGF-β activity through sustained activation by integrins[33].

Plasminogen activator inhibitor-1 is a biomarker for several vascular disease states, including diabetes [1, 3–5, 34–36] which is also associated with the disregulation of MEJs[18]. In C57Bl/6 mice fed a high fat diet there is a significant increase in body weight, blood glucose and PAI-1 levels, effectively mimicking diabetic conditions (Supplementary Fig IX). Isolated coronary arterioles from these mice have significantly more MEJs and decreased IEL thickness as compared to the C57Bl/6, so we determined if increases in circulating PAI-1 were capable of regulating MEJ formation in vivo using heterotypic heart transplants. When hearts from PAI-$1^{-/-}$ mice were transplanted into a C57Bl/6 mouse and exposed to circulating PAI-1, MEJ formation within PAI-$1^{-/-}$ coronary arterioles was significantly increased five days post surgery. We confirmed that changes in circulating PAI-1 affected MEJ formation by injecting rPAI-1 into PAI-$1^{-/-}$ mice, demonstrating an increase in MEJ formation in isolated coronary arterioles similar to that seen in PAI-$1^{-/-}$ vessel transplanted into a C57Bl/6 and C57Bl/6 controls. Evidence shows that increases in available PAI-1 coincides with increased cellular invasion[37] and our data supports a similar mechanism, whereby increases in MEJ formation occur in response to circulating PAI-1.

Application of rPAI-1 in vitro and heterotypic heart transplants suggest for the first time that increases in PAI-1 at the EC luminal membrane can effect MEJ formation. The application of biotin-conjugated rPAI-1 demonstrated the translocation of biotin-conjugated rPAI-1 from the luminal surface of EC to the MEJ and further supports the hypothesized movement of PAI-1. It is well documented that VSMC produce PAI-1[38, 39] and it is likely that some of the endogenous PAI-1 expressed at the MEJ is VSMC derived, however, the application of biotin-conjugated rPAI-1 to the VSMC monolayer showed no increase in PAI-1 at the MEJ, which coincides with experiments that show with application of mAb or rPAI-1 to the VSMC monolayer there is no change in the number of MEJs in vitro. Therefore, our data indicates that in conditions where circulating PAI-1 is increased, changes in MEJ formation are mediated through the movement of circulating PAI-1 from the luminal surface of ECs to the IEL. Although the internalization of PAI-1 for degradation occurs via a low density lipoprotein receptor mediated mechanism was first described in 1992[40, 41] , there is currently no defined mechanism for the uptake and translocation of circulating PAI-1 to areas of the IEL and subsequent sites of potential MEJ formation.

As a unique signaling microdomain, the MEJ is hypothesized to play a key role in the regulation of heterocellular $Ca^{2+}$ signaling (for review see18). Modulation of PAI-1 activity in vitro using rPAI-1or mAb to PAI-1 showed no variation in the maximal EC $Ca^{2+}$ responses following PE stimulation of VSMC. This indicated that the EC could still respond normally to second messengers that are produced in the VSMC and move through gap junctions at the MEJ (e.g., 30, 42). However, there was a significant difference in the rate of $Ca^{2+}$ response between VCCCs treated with rPAI-1 and those with depleted PAI-1, correlating with an increase or decrease (respectively) in the number of MEJs (Fig 7). We interpret these data to mean that the number of MEJs, specifically gap junctions at the MEJ, dictates the time necessary for EC to respond to second messengers from the VSMC.

In concurrence with our $Ca^{2+}$ data and the observed effects of PAI-1 on MEJ formation, we would hypothesize that mice deficient in PAI-1 have impaired vasoreactivity to agonist stimulation due to a reduced number of MEJs. Indeed, it was recently reported that mesenteric artery rings from PAI-$1^{-/-}$ mice have diminished sensitivity to acetylcholine (Ronald Korthuis, PhD, University of Missouri-Columbia, unpublished data, 2009). It is also well documented that in multiple diabetic models with upregulated PAI-1, there is increased sensitivity to vasoconstrictors (e.g. PE)[43–46]. Our data supports this hypothesis, providing a potential mechanism for how PAI-1 may affect vasoreactivity through changes in MEJ formation. However, it is important to note that despite increasing evidence supporting a role for MEJs in pathological conditions, it is still unknown if these changes are compensatory or promoting the disease state.

In conclusion, after isolating proteins expressed at the MEJ and performing 2D-DIGE analysis, we have identified PAI-1, an important mediator of ECM degradation and major biomarker for several vascular diseases, as being enriched at the MEJ. Our data suggests localization of PAI-1 to the MEJ allows it to act as a key regulator of MEJ formation and function. The increase or decrease in MEJs in response to changes in PAI-1, including conditions that mimic diabetes, correlate with altered temporal $Ca^{2+}$ responses in EC following VSMC stimulation. Although this paper does not present a mechanism for how PAI-1 regulates MEJ formation, it is the first evidence of a protein inducing the formation of MEJs, as is extensively demonstrated using innovative techniques both in vitro and in vivo. Although it remains to be seen if the changes in MEJ formation during vascular disease are beneficial, the accumulation of this work suggests that manipulation of PAI-1 at the MEJ may be an attractive pharmaceutical target to treat vascular associated diseases where heterocellular communication is aberrant.

**Novelty and Significance**

Myoendothelial junctions (MEJs) are predominantly located within the resistance vasculature and couple endothelial and vascular smooth muscle cells within the vessel wall. The MEJs are suggested to play a role in the regulation of vasoreactivity via heterocellular communication and have been implicated in several vascular diseases; however how these structures are regulated is currently unknown. The formation of cellular extensions is governed by plasminogen activator inhibitor-1 (PAI-1), which is a major biomarker for microvascular diseases. We have identified PAI-1 at the MEJ and show a direct correlation between PAI-1 and the number of MEJs. We demonstrate that PAI-1 directly regulates MEJ formation and notably, we show there is an increase in MEJs in conditions that mimic type II diabetes. Microvascular dysfunction associated with type II diabetes can lead to hypertensive conditions and our data show that increases in the number of MEJs results in increased sensitivity to vasoconstrictors *in vitro*. In sum, these data are the first to demonstrate the ability of a single protein to regulate MEJ formation and provide a potential future pharmaceutical target for microvascular diseases associated with increased PAI-1.

**What is known?**

- Plasminogen activator inhibitor-1 is a major biomarker for a variety of vascular pathologies and regulates the invasion of cellular extensions into the extracellular matrix.
- Myoendothelial junctions (MEJs) link endothelial and vascular smooth muscle cells and promote heterocellular communication within the resistance vasculature.
- Myoendothelial junctions are hypothesized to be associated with several vascular disease states.

**What new information does this article contribute?**

- Plasminogen activator inhibitor-1 expression is enriched at the MEJ *in vitro* and *in vivo*.
- The formation of MEJs is regulated by PAI-1 *in vitro* and *in vivo* and effects heterocellular $Ca^{2+}$ signaling at the MEJ *in vitro*.
- In mice fed a diabetogenic diet, increases in circulating PAI-1 resulted in increased MEJ formation.

## Supplementary Material

Refer to Web version on PubMed Central for supplementary material.

## Non-standard Abbreviations and Acronyms

| | |
|---|---|
| EC | endothelial cell(s) |
| VSMC | vascular smooth muscle cell(s) |
| MEJ | myoendothelial junction(s) |
| VCCC | vascular cell co-culture |
| PAI-1 | plasminogen activator inhibitor-1 |
| uPA | urokinase plasminogen activator |
| tPA | tissue plasminogen activator |

| | |
|---|---|
| ECM | extracellular matrix |
| IEL | internal elastic lamina |
| PE | phenylephrine |
| GA | glycyrrhetinic acid |

## Acknowledgments

We are grateful to Brian Duling, Scott Johnstone, Jeremy Ross and Jenny Han for critical reading and discussion of the manuscript; Jessica Connelly for the kind gift of human microvascular coronary artery cells; the University of Virginia Histology Core for sectioning of VCCCs; Jan Reddick and Stacey Guillford at the Advanced Microscopy Core for services relating to electron microscopy; and Hong Pei in the Robert M. Berne Cardiovascular Research Center Animal Surgery Core Facility. We also thank Thomas Geer (Olympus America) for valuable help in microscope design.

**Sources of Funding**

This work was supported by NIH HL088554 (BEI), an American Heart Association Scientist Development Grant (BEI), and NIH HL084422 (NL).

## Reference List

1. Alessi MC, Juhan-Vague I. Metabolic syndrome, haemostasis and thrombosis. Thromb Haemost 2008;99:995–1000. [PubMed: 18521499]
2. Lijnen HR. Pleiotropic functions of plasminogen activator inhibitor-1. J Thromb Haemost 2005;3:35–45. [PubMed: 15634264]
3. Brosius FC III. New insights into the mechanisms of fibrosis and sclerosis in diabetic nephropathy. Rev Endocr Metab Disord 2008;9:245–254. [PubMed: 18726161]
4. Eddy AA, Giachelli CM. Renal expression of genes that promote interstitial inflammation and fibrosis in rats with protein-overload proteinuria. Kidney Int 1995;47:1546–1557. [PubMed: 7643523]
5. Hirano T, Kashiwazaki K, Moritomo Y, Nagano S, Adachi M. Albuminuria is directly associated with increased plasma PAI-1 and factor VII levels in NIDDM patients. Diabetes Res Clin Pract 1997;36:11–18. [PubMed: 9187410]
6. Ellis V, Wun TC, Behrendt N, Ronne E, Dano K. Inhibition of receptor-bound urokinase by plasminogen-activator inhibitors. J Biol Chem 1990;265:9904–9908. [PubMed: 2161846]
7. Andreasen PA, Nielsen LS, Kristensen P, Grondahl-Hansen J, Skriver L, Dano K. Plasminogen activator inhibitor from human fibrosarcoma cells binds urokinase-type plasminogen activator, but not its proenzyme. J Biol Chem 1986;261:7644–7651. [PubMed: 3086313]
8. Eitzman DT, Westrick RJ, Nabel EG, Ginsburg D. Plasminogen activator inhibitor-1 and vitronectin promote vascular thrombosis in mice. Blood 2000;95:577–580. [PubMed: 10627465]
9. Pepper MS. Role of the matrix metalloproteinase and plasminogen activator-plasmin systems in angiogenesis. Arterioscler Thromb Vasc Biol 2001;21:1104–1117. [PubMed: 11451738]
10. Farrehi PM, Ozaki CK, Carmeliet P, Fay WP. Regulation of arterial thrombolysis by plasminogen activator inhibitor-1 in mice. Circulation 1998;97:1002–1008. [PubMed: 9529269]
11. Pepper MS, Montesano R. Proteolytic balance and capillary morphogenesis. Cell Differ Dev 1990;32:319–327. [PubMed: 1711917]
12. Stefansson S, Petitclerc E, Wong MK, McMahon GA, Brooks PC, Lawrence DA. Inhibition of angiogenesis in vivo by plasminogen activator inhibitor-1. J Biol Chem 2001;276:8135–8141. [PubMed: 11083866]
13. Montesano R, Pepper MS, Mohle-Steinlein U, Risau W, Wagner EF, Orci L. Increased proteolytic activity is responsible for the aberrant morphogenetic behavior of endothelial cells expressing the middle T oncogene. Cell 1990;62:435–445. [PubMed: 2379237]

14. Isogai C, Laug WE, Shimada H, Declerck PJ, Stins MF, Durden DL, Erdreich-Epstein A, DeClerck YA. Plasminogen activator inhibitor-1 promotes angiogenesis by stimulating endothelial cell migration toward fibronectin. Cancer Res 2001;61:5587–5594. [PubMed: 11454712]
15. Rhodin JA. The ultrastructure of mammalian arterioles and precapillary sphincters. J Ultrastruct Res 1967;18:181–223. [PubMed: 5337871]
16. Sandow SL, Hill CE. Incidence of myoendothelial gap junctions in the proximal and distal mesenteric arteries of the rat is suggestive of a role in endothelium-derived hyperpolarizing factor-mediated responses. Circ Res 2000;86:341–346. [PubMed: 10679487]
17. Taugner R, Kirchheim H, Forssmann WG. Myoendothelial contacts in glomerular arterioles and in renal interlobular arteries of rat, mouse and Tupaia belangeri. Cell Tissue Res 1984;235:319–325. [PubMed: 6705035]
18. Heberlein KR, Straub AC, Isakson BE. The Myoendothelial Junction: Breaking through the Matrix? Microcirculation 2009:1–16.
19. Fukao M, Hattori Y, Kanno M, Sakuma I, Kitabatake A. Alterations in endothelium-dependent hyperpolarization and relaxation in mesenteric arteries from streptozotocin-induced diabetic rats. Br J Pharmacol 1997;121:1383–1391. [PubMed: 9257918]
20. Makino A, Ohuchi K, Kamata K. Mechanisms underlying the attenuation of endothelium-dependent vasodilatation in the mesenteric arterial bed of the streptozotocin-induced diabetic rat. Br J Pharmacol 2000;130:549–556. [PubMed: 10821782]
21. Wigg SJ, Tare M, Tonta MA, O'Brien RC, Meredith IT, Parkington HC. Comparison of effects of diabetes mellitus on an EDHF-dependent and an EDHF-independent artery. Am.J.Physiol Heart Circ Physiol 2001;281:H232–H240. [PubMed: 11406490]
22. Isakson BE, Duling BR. Heterocellular contact at the myoendothelial junction influences gap junction organization. Circ Res 2005;97:44–51. [PubMed: 15961721]
23. Johnstone SR, Ross J, Rizzo MJ, Straub AC, Lampe PD, Leitinger N, Isakson BE. Oxidized phospholipid species promote in vivo differential cx43 phosphorylation and vascular smooth muscle cell proliferation. Am J Pathol 2009;175:916–924. [PubMed: 19608875]
24. Lecanda F, Towler DA, Ziambaras K, Cheng SL, Koval M, Steinberg TH, Civitelli R. Gap junctional communication modulates gene expression in osteoblastic cells. Mol Biol Cell 1998;9:2249–2258. [PubMed: 9693379]
25. Isakson BE, Best AK, Duling BR. Incidence of protein on actin bridges between endothelium and smooth muscle in arterioles demonstrates heterogeneous connexin expression and phosphorylation. Am J Physiol Heart Circ Physiol 2008;294:H2898–H2904. [PubMed: 18408134]
26. Niimi M. The technique for heterotopic cardiac transplantation in mice: experience of 3000 operations by one surgeon. J Heart Lung Transplant 2001;20:1123–1128. [PubMed: 11595568]
27. Isakson BE, Ramos SI, Duling BR. Ca2+ and inositol 1,4,5-trisphosphate-mediated signaling across the myoendothelial junction. Circ Res 2007;100:246–254. [PubMed: 17218602]
28. Mazzieri R, Masiero L, Zanetta L, Monea S, Onisto M, Garbisa S, Mignatti P. Control of type IV collagenase activity by components of the urokinase-plasmin system: a regulatory mechanism with cell-bound reactants. EMBO J 1997;16:2319–2332. [PubMed: 9171346]
29. Mars WM, Liu ML, Kitson RP, Goldfarb RH, Gabauer MK, Michalopoulos GK. Immediate early detection of urokinase receptor after partial hepatectomy and its implications for initiation of liver regeneration. Hepatology 1995;21:1695–1701. [PubMed: 7768515]
30. Isakson BE. Localized expression of an Ins(1,4,5)P3 receptor at the myoendothelial junction selectively regulates heterocellular Ca2+ communication. J Cell Sci 2008;121:3664–3673. [PubMed: 18946029]
31. Gils A, Pedersen KE, Skottrup P, Christensen A, Naessens D, Deinum J, Enghild JJ, Declerck PJ, Andreasen PA. Biochemical importance of glycosylation of plasminogen activator inhibitor-1. Thromb Haemost 2003;90:206–217. [PubMed: 12888867]
32. Brogren H, Sihlbom C, Wallmark K, Lonn M, Deinum J, Karlsson L, Jern S. Heterogeneous glycosylation patterns of human PAI-1 may reveal its cellular origin. Thromb Res 2008;122:271–281. [PubMed: 18508114]

33. Pedroja BS, Kang LE, Imas AO, Carmeliet P, Bernstein AM. Plasminogen activator inhibitor-1 regulates integrin alphavbeta3 expression and autocrine transforming growth factor beta signaling. J Biol Chem 2009;284:20708–20717. [PubMed: 19487690]
34. Goldberg RB. Cytokine and cytokine-like inflammation markers, endothelial dysfunction, and imbalanced coagulation in development of diabetes and its complications. J Clin Endocrinol Metab 2009;94:3171–3182. [PubMed: 19509100]
35. Festa A, Williams K, Tracy RP, Wagenknecht LE, Haffner SM. Progression of plasminogen activator inhibitor-1 and fibrinogen levels in relation to incident type 2 diabetes. Circulation 2006;113:1753–1759. [PubMed: 16585388]
36. Festa A, D'Agostino R Jr, Tracy RP, Haffner SM. Elevated levels of acute-phase proteins and plasminogen activator inhibitor-1 predict the development of type 2 diabetes: the insulin resistance atherosclerosis study. Diabetes 2002;51:1131–1137. [PubMed: 11916936]
37. Chazaud B, Ricoux R, Christov C, Plonquet A, Gherardi RK, Barlovatz-Meimon G. Promigratory effect of plasminogen activator inhibitor-1 on invasive breast cancer cell populations. Am J Pathol 2002;160:237–246. [PubMed: 11786417]
38. Dellas C, Loskutoff DJ. Historical analysis of PAI-1 from its discovery to its potential role in cell motility and disease. Thromb Haemost 2005;93:631–640. [PubMed: 15841306]
39. Demyanets S, Kaun C, Rychli K, Rega G, Pfaffenberger S, Afonyushkin T, Bochkov VN, Maurer G, Huber K, Wojta J. The inflammatory cytokine oncostatin M induces PAI-1 in human vascular smooth muscle cells in vitro via PI 3-kinase and ERK1/2-dependent pathways. Am J Physiol Heart Circ Physiol 2007;293:H1962–H1968. [PubMed: 17604327]
40. Herz J, Clouthier DE, Hammer RE. LDL receptor-related protein internalizes and degrades uPA-PAI-1 complexes and is essential for embryo implantation. Cell 1992;71:411–421. [PubMed: 1423604]
41. Nykjaer A, Petersen CM, Moller B, Jensen PH, Moestrup SK, Holtet TL, Etzerodt M, Thogersen HC, Munch M, Andreasen PA, et al. Purified alpha 2-macroglobulin receptor/LDL receptor-related protein binds urokinase.plasminogen activator inhibitor type-1 complex. Evidence that the alpha 2-macroglobulin receptor mediates cellular degradation of urokinase receptor-bound complexes. J Biol Chem 1992;267:14543–14546. [PubMed: 1378833]
42. Lamboley M, Pittet P, Koenigsberger M, Sauser R, Beny JL, Meister JJ. Evidence for signaling via gap junctions from smooth muscle to endothelial cells in rat mesenteric arteries: possible implication of a second messenger. Cell Calcium 2005;37:311–320. [PubMed: 15755492]
43. Su J, Lucchesi PA, Gonzalez-Villalobos RA, Palen DI, Rezk BM, Suzuki Y, Boulares HA. Matrougui K. Role of advanced glycation end products with oxidative stress in resistance artery dysfunction in type 2 diabetic mice. Arterioscler Thromb Vasc Biol 2008;28:1432–1438. [PubMed: 18483403]
44. Heyman SN, Hanna Z, Nassar T, Shina A, Akkawi S, Goldfarb M, Rosen S, Higazi AA. The fibrinolytic system attenuates vascular tone: effects of tissue plasminogen activator (tPA) and aminocaproic acid on renal microcirculation. Br J Pharmacol 2004;141:971–978. [PubMed: 14993107]
45. Khavandi K, Greenstein AS, Sonoyama K, Withers S, Price A, Malik RA, Heagerty AM. Myogenic tone and small artery remodelling: insight into diabetic nephropathy. Nephrol Dial Transplant 2009;24:361–369. [PubMed: 19028754]
46. Matsumoto T, Ishida K, Nakayama N, Kobayashi T, Kamata K. Involvement of NO and MEK/ERK pathway in enhancement of endothelin-1-induced mesenteric artery contraction in later-stage type 2 diabetic Goto-Kakizaki rat. Am J Physiol Heart Circ Physiol 2009;296:H1388–H1397. [PubMed: 19286964]

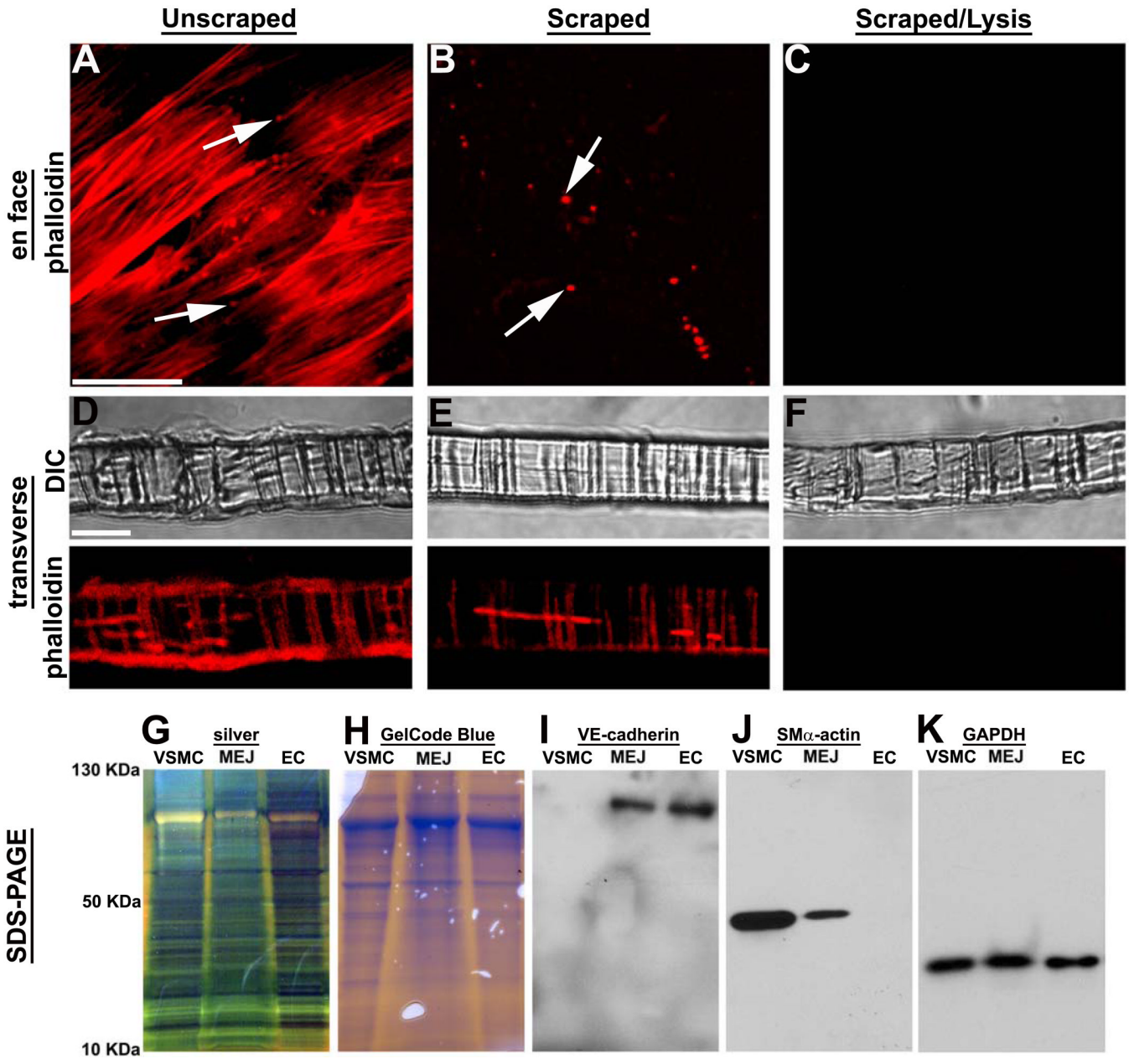


**Figure 1. Isolation of MEJ protein fractions from vascular cell co-culture**

Confocal microscopy of VCCC stained with phalloidin en face (A–C) and transverse (D–F). Conditions shown include unscraped membranes viewed en face (A) and transverse (D) scraped membranes viewed enface (B) and transverse (E) as well as scraped and lysed membranes viewed en face (C) and transverse (F). SDS-PAGE of VSMC, EC and MEJ fractions stained with GelCode Blue (G) and silver stain (H). Immunoblots of protein fractions probed for VE-Cadherin (I), SMα-actin (J) and GAPDH (K). Bar in A is 20 μm and representative for A–C; bar in D is 10 μm and representative for D–F. Arrows in A and B indicate pores of the Transwell insert.

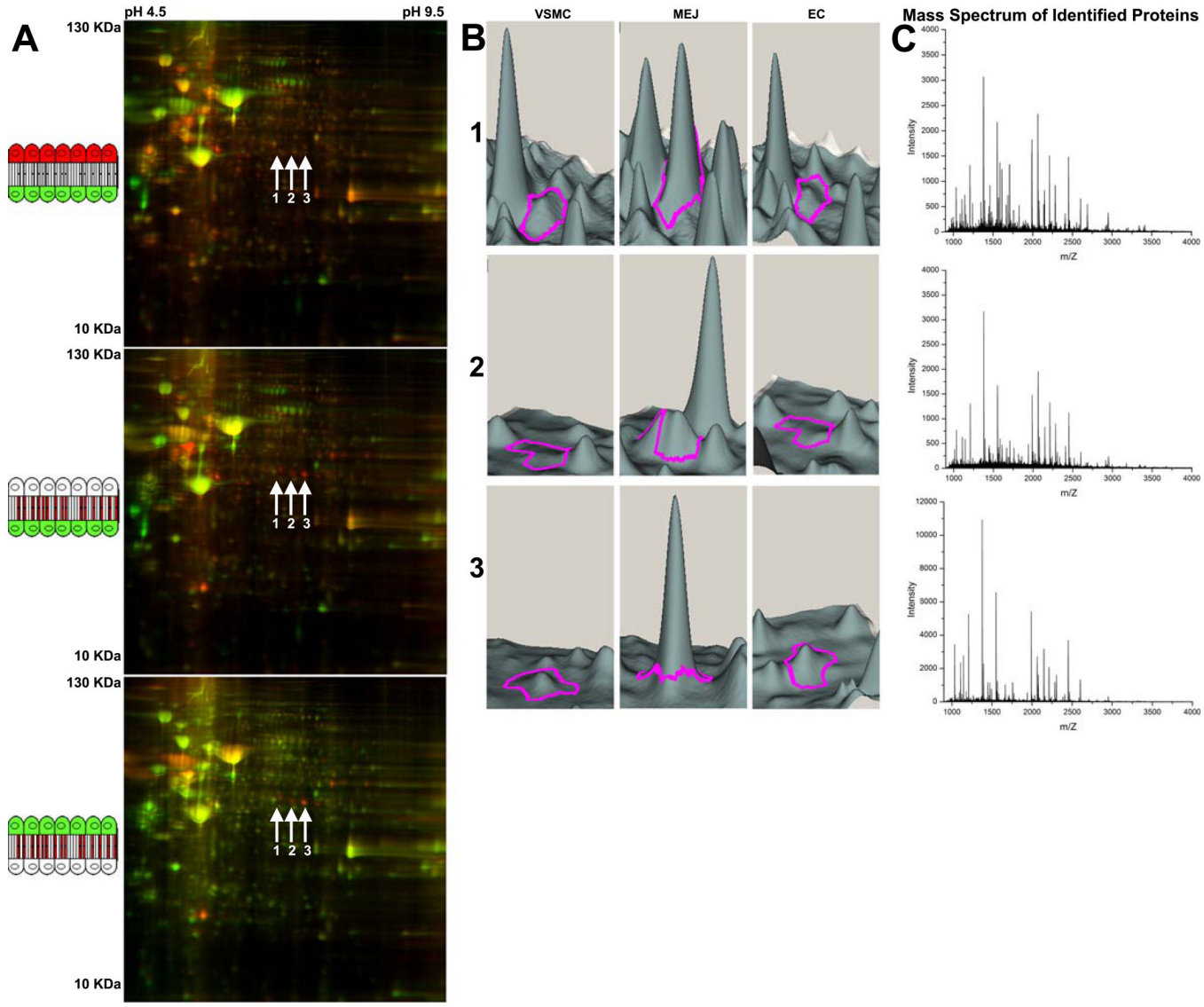


**Figure 2. 2D-DIGE analysis of isolated MEJ protein fractions from vascular cell co-culture**

2D-DIGE blots of isolated protein fractions from the VCCC. Cartoon schematics in A represent the compared fractions for each gel image as they occur in the VCCC. Conditions include comparison of EC (red) to VSMC (green), (A, top); MEJ (red) to VSMC (green), (A, middle); and MEJ (red) to EC (green), (A, bottom). Arrows labeled 1–3 in A indicate three spots representing a unique protein with greater than 2.5 fold increase in fluorescent intensity (i.e., protein expression) in the MEJ versus VSMC and EC fractions. Using Quantitative DeCyder analysis, spots 1–3 are represented in a 3D visualization for each spot of interest and identified by a magenta tracer (Fig 2B), indicating protein fluorescent intensity peaks in VSMC, MEJ and EC fractions. The mass spectrum of spots 1 (C, top), 2 (C, middle) and 3 (C, bottom) identified each spot as plasminogen activator inhibitor-1. For all images, n=30 Tranwells.

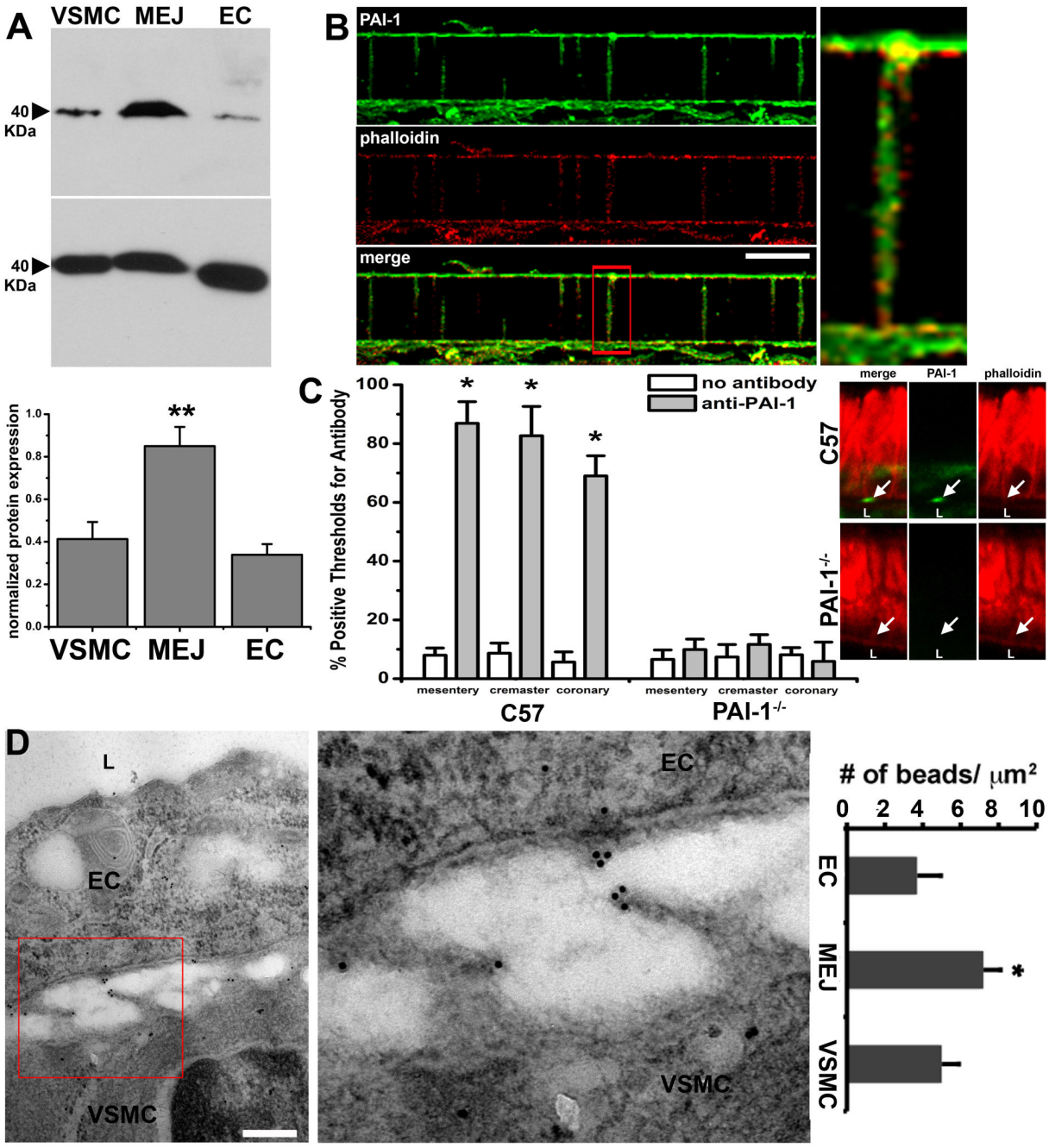


**Figure 3. Localization of PAI-1 at the MEJ**

Immunoblots of VSMC, EC and MEJ fractions isolated from the VCCC blotted for PAI-1 and GAPDH as a loading control. Normalized quantification of protein expression for PAI-1 in each fraction is given in the adjacent histogram, n=4 (A). Immunocytochemistry of a single focal plane of a transverse section of the VCCC labeled for PAI-1 (green) and actin (red; phalloidin) demonstrate colocalized expression of both proteins regardless of the location in the Transwell pores (B). In vivo, the expression of PAI-1 on actin bridges that form between EC and VSMC (i.e. MEJs) in mesentery, cremaster and coronary microvascular beds is quantified using confocal microscopy in both C57Bl/6 and PAI-$1^{-/-}$ mice, n=3 mice per experimental paradigm, 5 images per mouse (C). A representative TEM image of a MEJ from

a mouse coronary arteriole labeled for PAI-1 with 10 nm gold particles is shown and quantified as number of beads per micrometer squared in D, n=3 mice per experimental paradigm, 5 images per mouse. Enlargement of white box in B is shown on right. In C, arrow indicates PAI-1 labeling. In D, “L” indicates lumen. Enlargement of red box insert in D is shown on right. Bar in B is 5 μm, bar in D is 0.5 μm, * $p<0.05$.

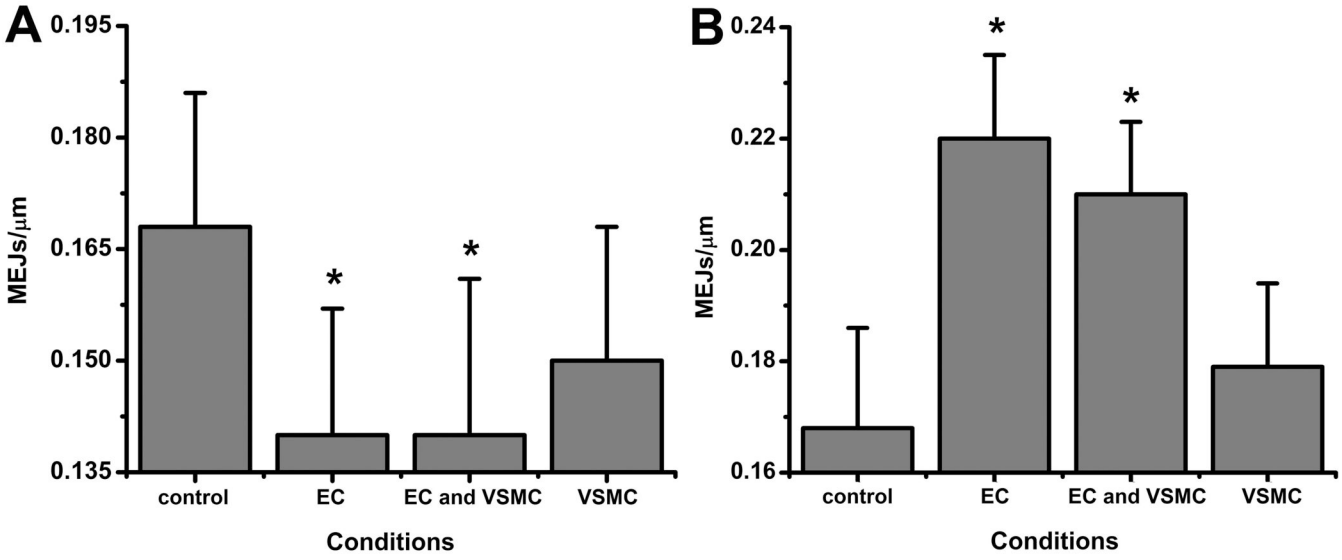


**Figure 4. Effects of PAI-1 on MEJ formation in vitro**

Metamorph analysis of changes in the number of MEJs per micrometer following inhibition of PAI-1 activity by application of 10 μg/mL PAI-1 specific mAb to the EC, EC and VSMC or VSMC monolayers is shown in A. Analysis of changes in the number of MEJs per micrometer following increases in PAI-1 activity by application of 0.1 μg/mL rPAI-1 to the EC, EC and VSMC or VSMC monolayers is shown in B. * $p<0.05$. For each condition (A–B), n=7 Transwells per condition, 10 images per Transwell.

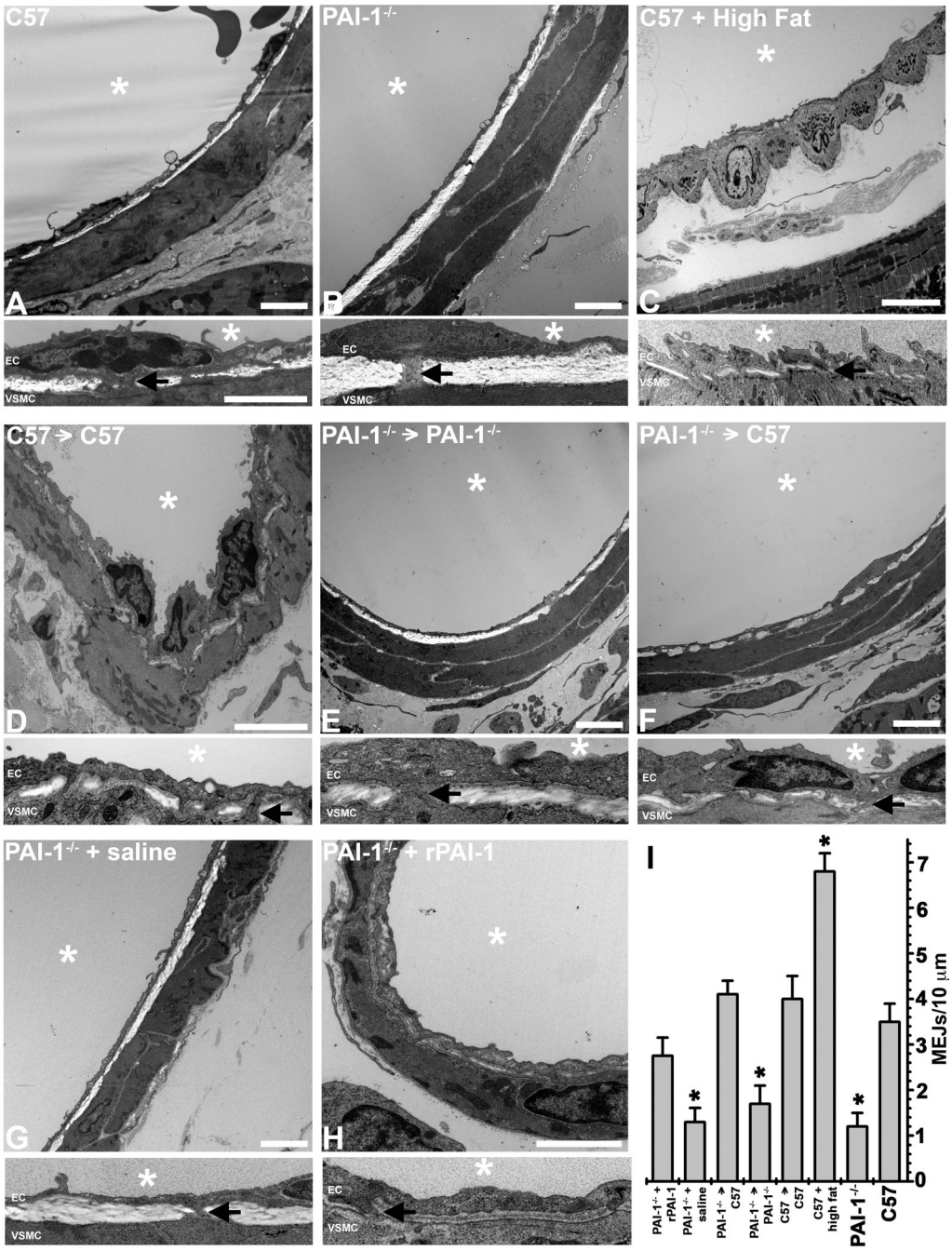


**Figure 5. Effects of PAI-1 on MEJ formation in vivo**

Ultrastructural TEM images of coronary arterioles at low magnification (top) and higher magnification (bottom) from C57Bl/6 (A), PAI-1$^{-/-}$ hearts (B) and C57Bl/6 fed a high fat western diet (C). TEM was used to visualize MEJs in coronary arterioles for each of the following experimental paradigms: C57Bl/6 hearts transplanted into recipient C57Bl/6 mice (D), PAI-1$^{-/-}$ hearts transplanted into recipient PAI-1$^{-/-}$ mice (E) and PAI-1$^{-/-}$ hearts transplanted into recipient C57Bl/6 mice (F). TEM analysis of coronary arterioles isolated from saline injected PAI-1$^{-/-}$ mice (G) and rPAI-1 injected PAI-1$^{-/-}$ mice (E) are also shown. The number of MEJS per 10μm radially is quantified for images A-H in (I). Bar in each low magnification image (top image) is 2 μm, bar in A (higher magnification, top) is 2 μm and

representative for all higher magnification images. In all images, * denotes vessel lumen and for each image, the lumen is located above the EC monolayer. EC and VSMC monolayers are separated by IEL for all images, arrows indicate MEJ in each magnified image. In I, *$p<0.05$ when compared to C57 animals. For images A–F,H, n=3 mice per experimental paradigm, 5 images per mouse. In G, n=2 mice, 5 images per mouse.

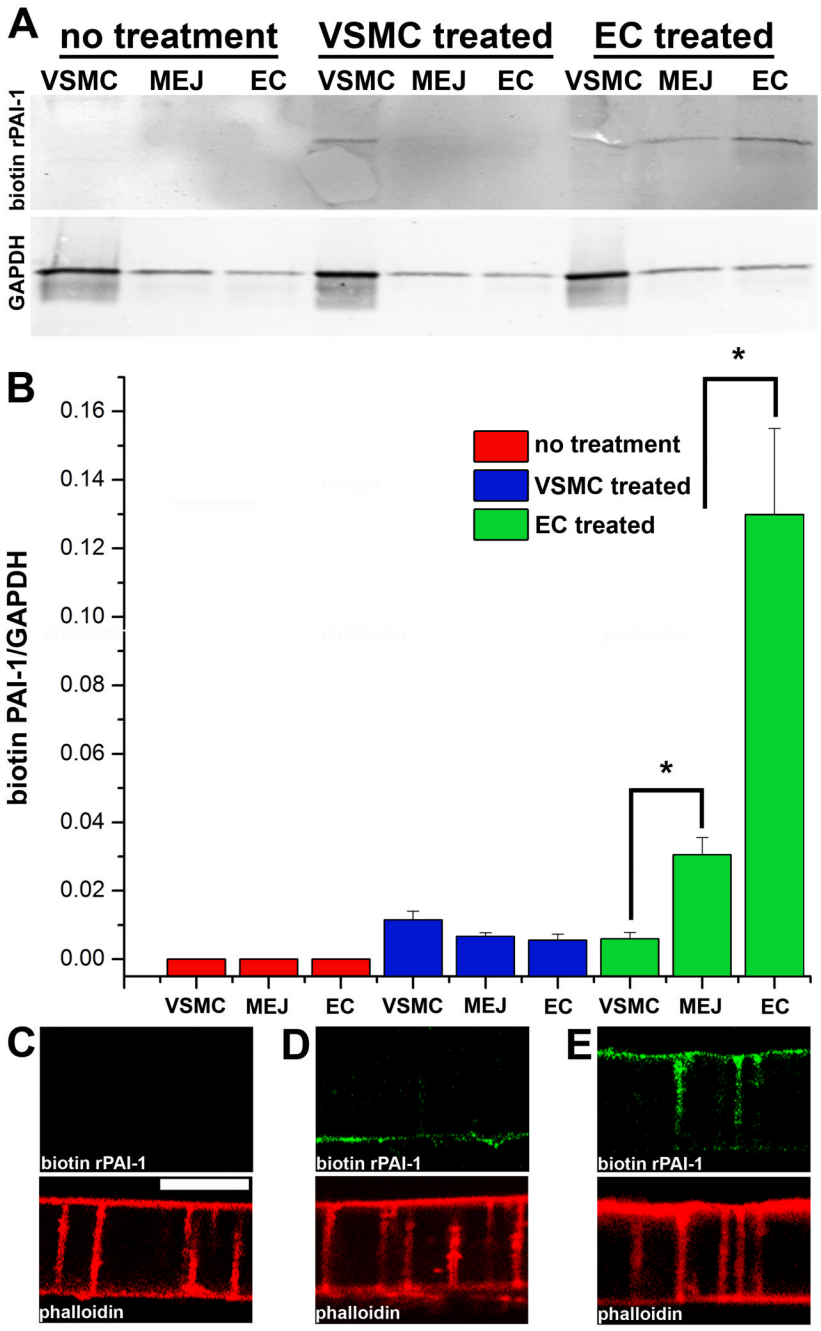


**Figure 6. Uptake and expression of biotin-conjugated rPAI-1 at the MEJ**

Immunoblots of VSMC, MEJ and EC fractions isolated from the VCCC stained with streptavidin. Three experimental paradigms were tested: no application of biotin-conjugated rPAI-1, application of biotin-conjugated rPAI-1 (0.1μg) to the VSMC monolayer and application of biotin-conjugated rPAI-1 (0.1μg) to only the EC monolayer. GAPDH is shown directly below each condition (A). Normalized quantification of protein expression for biotin-conjugated rPAI-1 for each fraction and experimental paradigm is given in (B). Immunocytochemistry on transverse sections of the VCCC for biotin-conjugated rPAI-1 using streptavidin (green) and F-actin (with phalloidin, red) for the following experimental paradigms: no application of biotin-conjugated rPAI-1, application of biotin-conjugated

rPAI-1 (0.1μg) to the VSMC monolayer and application of biotin-conjugated rPAI-1 (0.1μg) to only the EC monolayer). For all images, VCCC were treated 30 minutes prior to isolation. Bar in C is 10 μm and representative for images (C-D). *$p<0.05$. For A–B, n=4.

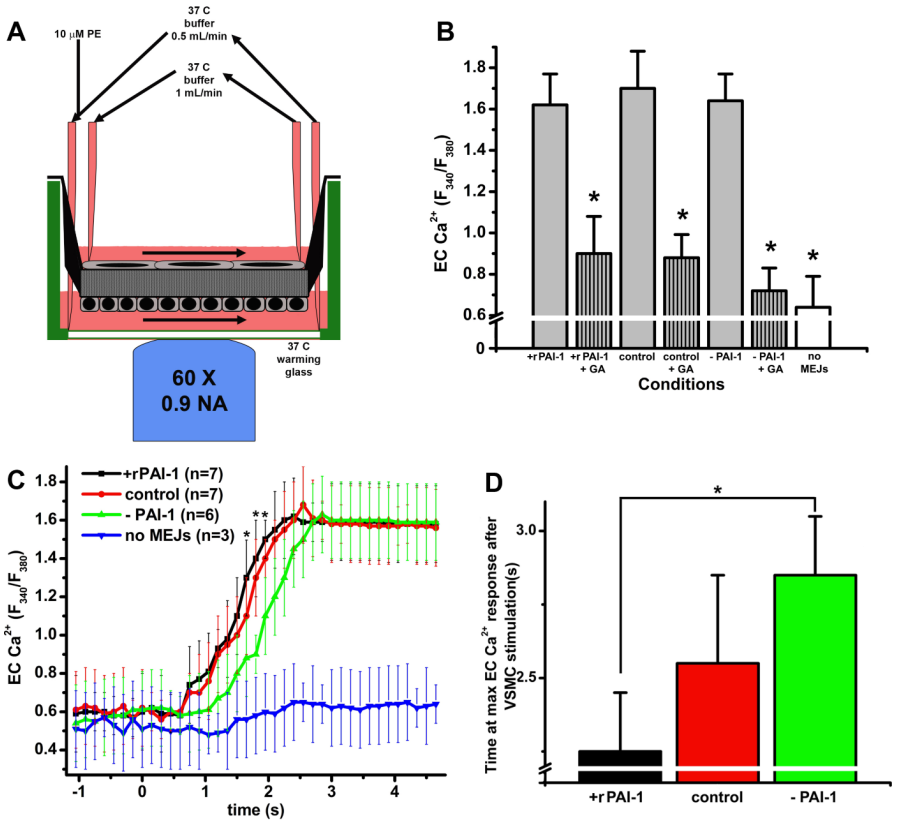


**Figure 7. Heterocellular $Ca^{2+}$ communication in vascular cell co-cultures with increases and decreases in PAI-1 activity**

Schematic representing the setup for measuring EC $[Ca^{2+}]_i$ following PE stimulation of the VSMC (A). The maximum values of EC $[Ca^{2+}]_i$ following PE stimulation is quantified and conditions include application of PAI-1 (+ rPAI-1); application of rPAI-1 + glycyrrhetinic acid (+ rPAI-1 + GA); control; control +GA, decreases in PAI-1 using a mAb against PAI-1, (−PAI-1); decreases in PAI-1 + glycerrhitinic acid (−PAI-1 + GA); and no MEJs (B). In C the temporal change in EC $[Ca^{2+}]_i$ after stimulation of VSMC with PE following application of rPAI-1 (+ rPAI-1), control; decreases in (− PAI-1); and no MEJs are shown. The time required to reach maximum EC $[Ca^{2+}]_i$ fluorescent intensity after VSMC stimulation with PE is shown for each condition: application of rPAI-1 (+ rPAI); control; and decreases in PAI-1 (−PAI-1) (D). For all images, VCCC were treated for the final 48 hours of culture, *p<0.05. n=3 Transwells per experimental condition.